Journal of Electroanalytical Chemistry 625 (2009) 27–32

Contents lists available at ScienceDirect

Journal of Electroanalytical Chemistry

journal homepage: www.elsevier.com/locate/jelechem

Electrocatalytic oxidation and reduction of H_2O_2 on vertically aligned Co_3O_4 nanowalls electrode: Toward H_2O_2 detection

Wenzhao Jia [a,1], Min Guo [b,1], Zhe Zheng [c], Ting Yu [c], Edgar G. Rodriguez [a], Ying Wang [a], Yu. Lei [a,*]

[a] Department of Chemical, Materials and Biomolecular Engineering, University of Connecticut, 191 Auditorium Road, Unit 3222, Storrs, CT 06269-3222, United States
[b] School of Electrical and Electronic Engineering, Nanyang Technological University, Nanyang Avenue, Singapore 639798, Singapore
[c] Division of Physics and Applied Physics, School of Physical and Mathematical Sciences, Nanyang Technological University, Singapore 637371, Singapore

ARTICLE INFO

Article history:
Received 8 April 2008
Received in revised form 23 September 2008
Accepted 30 September 2008
Available online 17 October 2008

Keywords:
Cobalt oxide
Nanowalls
Reduction
Oxidation
H_2O_2

ABSTRACT

Single crystal and vertically aligned cobalt oxide (Co_3O_4) nanowalls were synthesized by directly heating Co foil on a hot-plate under ambient conditions. The vertically aligned Co_3O_4 nanowalls grown on the plate show excellent mechanical property and were facilely attached to the surface of a glassy carbon (GC) electrode using conductive silver paint. The prepared Co_3O_4 nanowalls electrode was then applied to study the electrocatalytic oxidation and reduction of hydrogen peroxide (H_2O_2) in 0.01 M pH 7.4 phosphate buffer medium. Upon the addition of H_2O_2, the Co_3O_4 nanowalls electrode exhibits significant oxidation and reduction of H_2O_2 starting around +0.25 V (vs. Ag/AgCl), while no obvious redox activity is observed at a bare GC electrode over most of the potential range. The superior electrocatalytic response to H_2O_2 is mainly attributed to the large surface area, minimized diffusion resistance, high surface energy, and enhanced electron transfer of the as-synthesized Co_3O_4 nanowalls. The same Co_3O_4 nanowalls electrode was also applied for the amperometric detection of H_2O_2 and showed a fast response and high sensitivity at applied potentials of +0.8 V and −0.2 V (vs. Ag/AgCl), respectively. The results also demonstrate that Co_3O_4 nanowalls have great potential in sensor and biosensor applications.

Published by Elsevier B.V.

1. Introduction

Due to its strong oxidizing property, hydrogen peroxide (H_2O_2) is widely used in many fields. For example, H_2O_2 is useful for the synthesis of various organic compounds, food production, pulp and paper bleaching, sterilization, and clinical applications [1,2]. H_2O_2 is also used as an oxidant for many liquid-based fuel cells [3–9], and is readily present in a variety of commercial products such as cosmetic and pharmaceutical products [10,11]. Further, H_2O_2 has emerged as an important by-product of enzymatic reactions in the field of biosensing [12–19]. Thus, the detection and quantification of H_2O_2 remains a significant endeavor in a variety of fields.

Many analytical methods have been developed for the detection and quantification of H_2O_2 [11]. Among them, titration [20], spectrophotometric [21–23], fluorometric [24–28], chemiluminescent [29–31], and chromatographic [32–34] techniques are well known. However, electrochemical methods have emerged as preferable, owing to their relatively low cost, efficiency, high sensitivity, and ease of operation [35–37]. Different materials, such as noble metals, macrocycle complex of transition metals, carbon nanotubes, and enzymes have been used to modify electrodes for the reduction/oxidation as well as the detection of H_2O_2 [1,37–46]. In recent years, new efforts have been emphasized on the use of novel metal oxides nanomaterials to modify electrode surfaces for enhanced oxidation/reduction and sensitive detection of H_2O_2 because metal oxide nanomaterials are easy to be synthesized, have very high surface to volume ratio, and show great potential to enhance electrocatalytic activity and promote electron-transfer reactions at a lower overpotential [1,11,47,48].

Recently, several metal oxide nanomaterials have been deposited on the surface of electrodes and investigated for the reduction/oxidation and detection of H_2O_2. Cobalt oxide (Co_3O_4) [11,47] and copper oxide (CuO) nanoparticles [48] have been proved to perform well as H_2O_2 reduction catalysts in strong basic solution, as both Co_3O_4 and CuO are useful for transferring electrons between H_2O_2 and an electrode while enabling regeneration after electron exchanges with H_2O_2. However, the nanoparticles cannot stand alone and require, for example, a matrix to entrap them for electrode attachment. A major disadvantage of entrapment of metal oxide nanoparticles is the additional diffusion resistance offered by the entrapment material. Additionally, the strong basic solution (0.1–3 M NaOH) used in these studies greatly limits their application. The direct electrodeposition of cobalt oxide nanoparticles on the surface of a glassy carbon (GC) electrode has also been used to yield both particles with an average size of

* Corresponding author. Tel.: +1 860 486 4554.
E-mail address: ylei@engr.uconn.edu (Yu. Lei).
[1] Equal contribution.

0022-0728/$ - see front matter Published by Elsevier B.V.
doi:10.1016/j.jelechem.2008.09.020

100 nm and large agglomerated particles (~200–600 nm) [1]. The modified rotating electrode (2000 rpm) was then applied to the sensitive detection of H_2O_2 based on the oxidation current at +0.75 V (vs. Ag/AgCl). Even though the performance of the system is impressive, the needs for a rotating electrode and for more work to produce uniform particles with smaller size may limit its further application. Therefore, there remains a need for simpler processes to fabricate novel metal oxide nanomaterials with superior catalytic property for fast, sensitive, reliable, and stable detection of H_2O_2. Preferably, the novel metal oxide nanomaterials are free-standing, have excellent mechanical and electrocatalytic properties, and can be easily manipulated and attached to an electrode surface without the help of an entrapment matrix.

In this communication, we reported the synthesis of single crystal and vertically aligned cobalt oxide nanowalls, the fabrication of Co_3O_4 nanowalls electrode, and its application in the electrocatalytic oxidation and reduction of H_2O_2 in 0.01 M pH 7.4 phosphate buffer. The same electrode was also applied for the sensitive amperometric detection of H_2O_2 based on the oxidation and reduction currents at applied potentials of +0.8 V and −0.2 V (vs. Ag/AgCl), respectively. The as-prepared Co_3O_4 nanowalls show excellent mechanical and electrocatalytic properties, and have great potential for applications in electrochemical detection.

2. Experimental

2.1. Chemical and reagents

Co foil (0.1 mm thick, 99.95%) was purchased from Sigma–Aldrich. H_2O_2, Na_2HPO_4, and NaH_2PO_4 were obtained from Fisher. De-ionized water generated by a Barnstead water system was used to prepare aqueous solution. Conductive silver paint and nail enamel were bought from Structure Probe and Walmart, respectively.

2.2. Synthesis of vertically aligned Co_3O_4 nanowalls and preparation of Co_3O_4 nanowalls electrode

Our previously developed hot-plate technique was employed to fabricate vertically aligned Co_3O_4 nanowalls on Co substrate [49,50]. Briefly, pre-polished and cleaned Co foil was heated on a

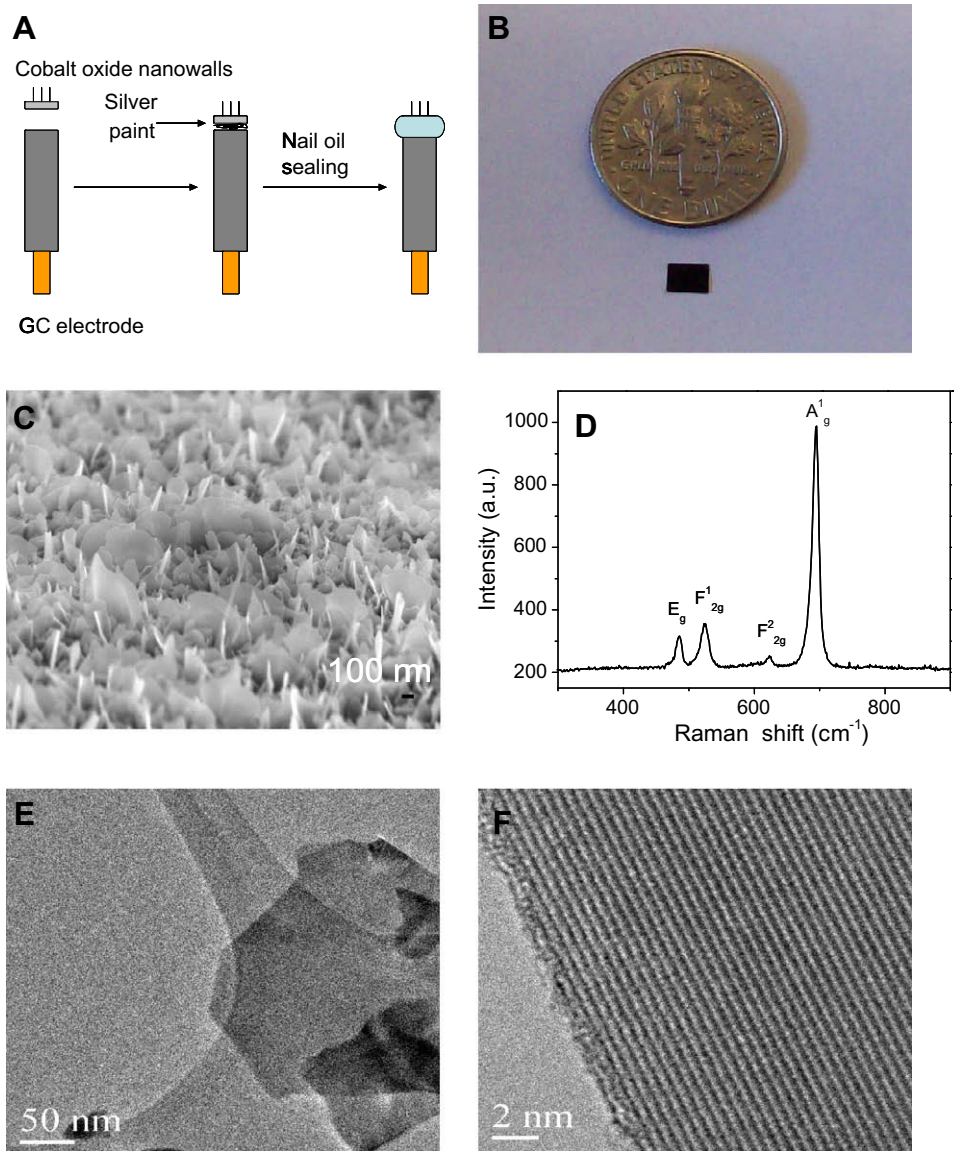

Fig. 1. (A) A schematic of the fabrication of Co_3O_4 nanowalls electrode; (B) an optical image of the as-grown Co_3O_4 nanowalls; (C) a typical SEM image of vertically aligned Co_3O_4 nanowalls; (D) micro-Raman spectrum of the Co_3O_4 nanowalls; (E) a typical TEM image of the Co_3O_4 nanowall; and (F) a HRTEM image of the Co_3O_4 nanowall.

hot-plate in an ambient condition. The heating temperature and duration were maintained at 300 °C and 5 h, respectively. After the growth, the shiny surface of metallic foils became dull and darkened, and the surface was fully covered with a large amount of vertically aligned nanowalls. Scanning electron microscopy (SEM; JEOL JSM-6700F), high-resolution transmission electron microscopy (HRTEM; JEOL JEM-2010F), and micro-Raman spectroscopy (ISA T64000 Triple Grating System) were used to characterize the morphology of the as-grown Co_3O_4 nanostructures.

To fabricate the electrode, the vertically aligned Co_3O_4 nanowalls film was cut to the desired size using scissors and attached to the surface of a GC electrode using conductive silver paint. Nail enamel was used to insulate the edge of substrate and the GC electrode. Therefore, only the vertically aligned Co_3O_4 nanowalls are exposed to the environment and the exposure area has a size of 3 mm × 2 mm. For comparison, the GC electrode with a diameter of 3 mm was used as a control. Fig. 1A shows a schematic of the electrode fabrication.

2.3. Apparatus and measurements

Cyclic voltammetric (CV) measurements were performed using an electrochemical workstation (Bio-logic SA VMP2) in a conventional three-electrode configuration, including a working electrode (Co_3O_4 nanowalls electrode or a bare GC electrode), an Ag/AgCl reference electrode, and a platinum counter electrode. H_2O_2 measurement was carried out in 0.01 M pH 7.4 phosphate buffer at room temperature. For amperometric detection, all measurements were performed by applying an appropriate potential (vs. Ag/AgCl) to the working electrode and allowing the transient background current to decay to a steady-state value, prior to the addition of H_2O_2. The current response due to the addition of H_2O_2 was recorded. A stirred solution was employed to provide convective transport.

3. Results and discussion

An optical image of the as-prepared Co_3O_4 nanowalls with size of 4 mm × 3 mm is shown in Fig. 1B. The size of vertically aligned Co_3O_4 nanowalls film is solely dependent on the size of the Co substrate used. The Co_3O_4 nanowalls film shows excellent mechanical properties and can be easily manipulated using tweezers and cut to small pieces using scissors. The typical morphology of the as-prepared Co_3O_4 nanowalls is presented in Fig. 1C. One can see that the surface is fully covered with a large amount of vertically aligned nanowall-like morphologies, forming porous 3D nanostructures. The thickness of the nanowalls is around 25 nm and the edges of the nanowalls are irregular. Typical Raman spectrum of the sample collected from the surface layer is shown in Fig. 1D. There are four peaks at 483, 523, 621, and 694 cm^{-1}, which correspond to E_g, F^1_{2g}, F^2_{2g}, and A^1_g modes of the crystalline Co_3O_4, indicating the surface layer is fully covered by Co_3O_4. The detailed structure of an individual Co_3O_4 nanowall is studied by TEM. Fig. 1E shows a typical TEM image of an individual Co_3O_4 nanowall while Fig. 1F displays a HRTEM image taken near the edge of an individual Co_3O_4 nanowall. The spacing of the lattice planes 0.472 nm corresponds to the interspacing of $(\bar{1}\bar{1}1)$ plane of Co_3O_4. The Raman spectrum and HRTEM images reveal that Co_3O_4 nanowalls are single crystalline.

The electrocatalytic property of the as-prepared Co_3O_4 nanowalls electrode was studied using cyclic voltammogram (CV). H_2O_2 was selected as a model compound in this study because the detection of H_2O_2, a product of enzymatic reactions catalyzed by a large number of oxidases (e.g. glucose oxidase and peroxidase), is practically important in the field of biosensor development [1]. Fig. 2 presents the CVs in the absence and presence of 10 mM H_2O_2, recorded at Co_3O_4 nanowalls electrode and the bare GC electrode, respectively. The scan rate is 50 mV/s. There are fun-

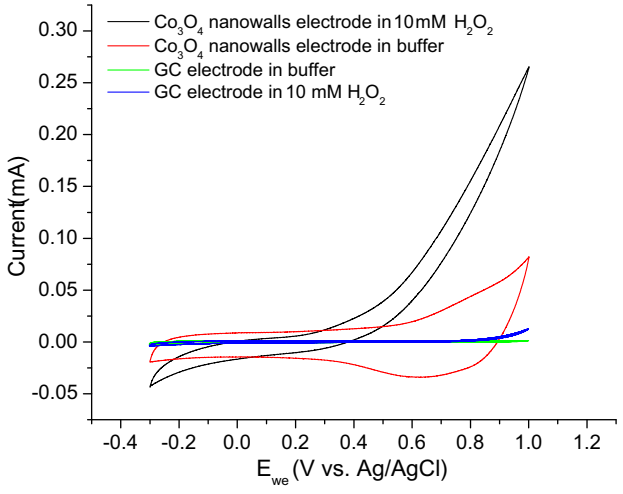

Fig. 2. Cyclic voltammograms of the Co_3O_4 nanowalls electrode and the bare GC electrode in 0.01 M pH 7.4 phosphate buffer in the absence and presence of 10 mM H_2O_2, respectively. Scan rate = 50 mV/s.

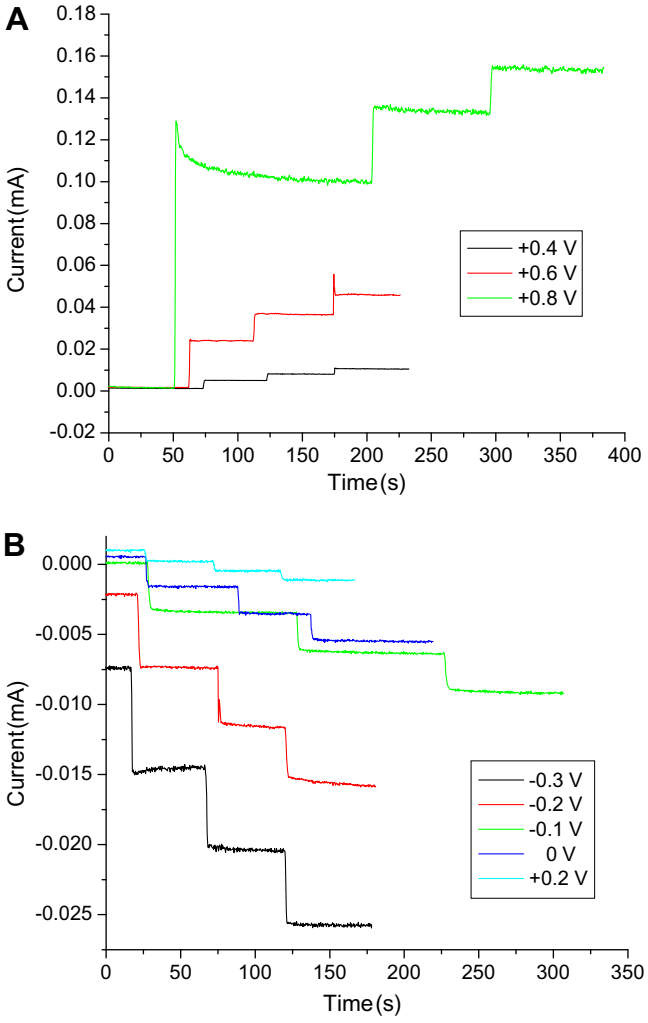

Fig. 3. Electrocatalytic oxidation (A) and reduction (B) of H_2O_2 on the Co_3O_4 nanowalls electrode at different applied potentials (vs. Ag/AgCl).

damental differences in the CVs. Only a small background current was observed at the bare GC electrode in buffer, while a dramatic increase of current signal toward the positive and negative ends of the potential range was observed when Co_3O_4 nanowalls electrode was used in buffer. This indicates that Co_3O_4 nanowalls electrode has excellent electrochemical properties, which may be attributed to the large surface area, high surface energy, and enhanced electron transfer of as-synthesized Co_3O_4 nanowalls. Upon the addition of 10 mM H_2O_2, the Co_3O_4 nanowalls electrode exhibits significant oxidation and reduction of H_2O_2 starting around +0.25 V (vs. Ag/AgCl), which can be attributed to the excellent electrocatalytic property of Co_3O_4 nanowalls. In contrast, no obvious redox activity is observed at the bare GC electrode over most of the potential range. The enhanced performance for H_2O_2 oxidation and reduction on Co_3O_4 nanowalls electrode may be due to an increase in the rate of electron transfer from H_2O_2 to the Co_3O_4 nanowalls, excellent accessibility of many nanoscale transport channels, as well as an improved reversibility of electron-transfer process on the Co_3O_4 nanowalls. The Co_3O_4 nanowalls electrode offers a marked decrease in the overvoltage for hydrogen peroxide oxidation and reduction, which enables convenient low-potential amperometric detection.

In order to study the effect of applied potentials on electrocatalytic oxidation and reduction of H_2O_2 at the Co_3O_4 nanowalls electrode, the amperometric responses to three successive additions of 1 mM H_2O_2 were recorded with respect to different applied potentials (Fig. 3). As both the oxidation and reduction of H_2O_2 at the Co_3O_4 nanowalls electrode start around +0.25 V and increase significantly towards the positive and negative ends, respectively, small stepwise current responses to H_2O_2 at +0.4 V (oxidation) and +0.2 V (reduction) were observed as expected (Fig. 3). In addition, the oxidation currents increase sharply with further increase of applied potentials and the similar trend is observed for the reduction currents with further decrease of applied potentials. The amperometric results match the CVs results well.

The superior electrocatalytic ability and easy manipulation makes the as-prepared vertically aligned Co_3O_4 nanowalls as an excellent electrochemical sensing platform for H_2O_2 detection. Fig. 4A shows typical amperometric responses of the Co_3O_4 nanowalls electrode to the successive addition of H_2O_2 at an applied potential of +0.8 V. The corresponding calibration curve is presented in Fig. 4B. The Co_3O_4 nanowalls electrode responds rapidly to the changes in H_2O_2 concentration, producing steady-state signals within 10 s. The calibration curve is linear up to 1.4 mM (the linear fitting correction coefficient $R = 0.9806$), with a sensitivity of 100.3 μA mM^{-1} (or 1671 μA mM^{-1} cm^{-2}) and a detection limit of 2.8 μM (a signal-to-noise of 3). Even though the sensitivity and fast response of Co_3O_4 nanowalls electrode is impressive at the applied

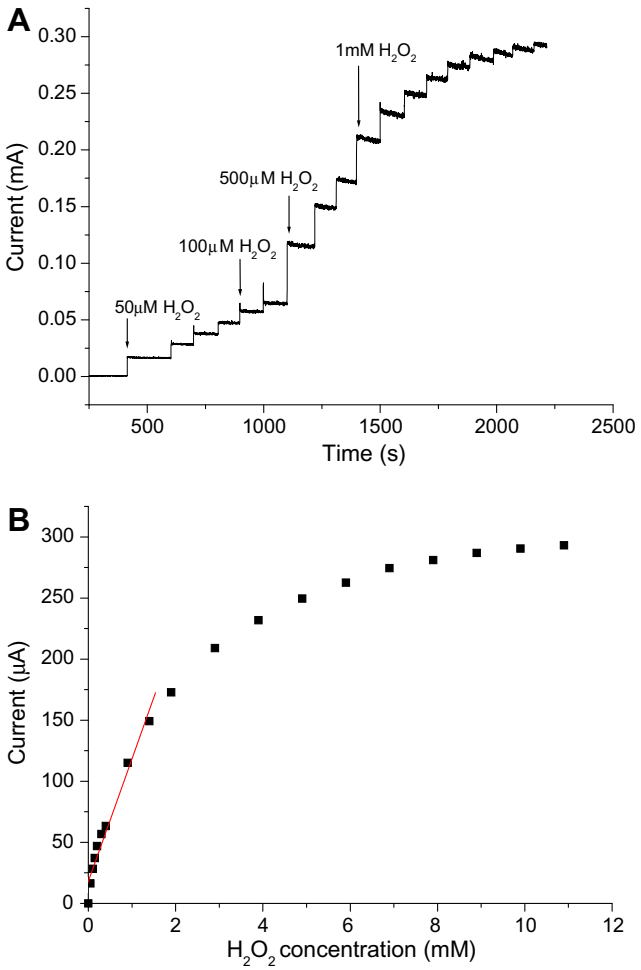

Fig. 4. Amperometric response of the Co_3O_4 nanowalls electrode with successive additions of H_2O_2 to 0.01 M pH 7.4 phosphate buffer at an applied potential of +0.8 V (vs. Ag/AgCl) and its corresponding calibration plot.

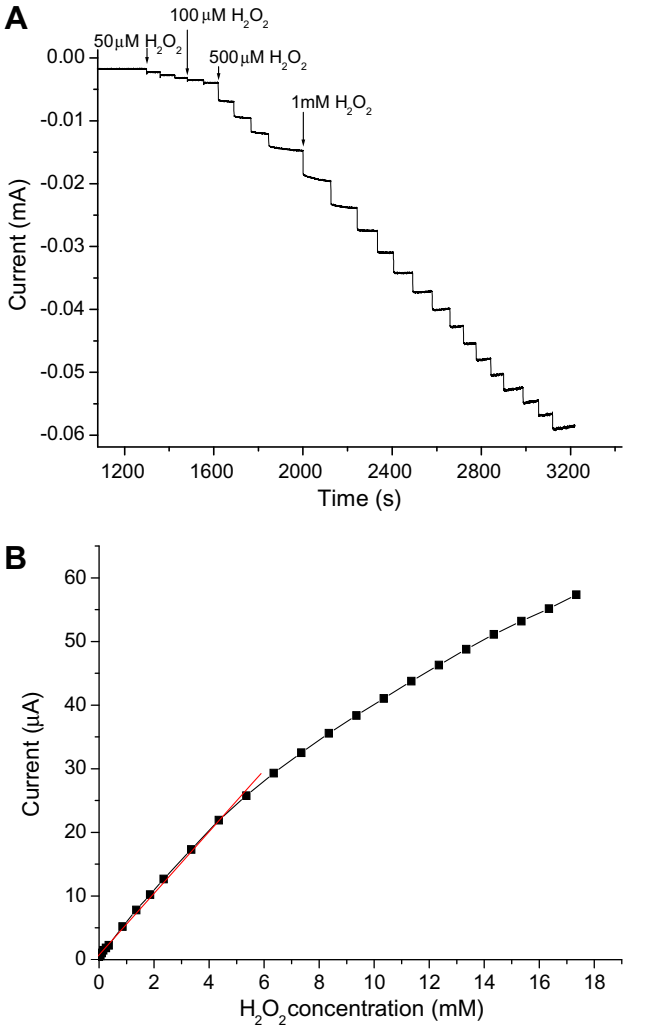

Fig. 5. Amperometric response of the Co_3O_4 nanowalls electrode with successive additions of H_2O_2 to 0.01 M pH 7.4 phosphate buffer at an applied potential of −0.2 V (vs. Ag/AgCl) and its corresponding calibration plot.

potential of +0.8 V, many compounds (e.g. acetaminophen, uric acid, and ascorbic acid) can be oxidized at such high applied potential and potentially interfere the detection of H_2O_2 in real samples. It has been reported that such interference can be significantly reduced when a lower applied potential is used. In order to minimize the biases from the potential interferences presented in the real samples, the possibility to perform amperometric detection of H_2O_2 based on the reduction at a lower applied potential was also investigated. Fig. 5A shows the amperometric response of the Co_3O_4 nanowalls electrode to the successive injection of H_2O_2 at an applied potential of −0.2 V. An applied potential of −0.2 V is chosen because the oxygen reduction can be eliminated. As shown in Fig. 5A, a well-defined response was observed during the successive additions of 50 μM, 100 μM, 500 μM, and 1 mM of H_2O_2, respectively. These results demonstrate a stable and efficient catalytic property of Co_3O_4 nanowalls. It can also be observed the Co_3O_4 nanowalls electrode responds rapidly to the change of H_2O_2 concentration and reaches the steady-state current within 10 s. The corresponding calibration curve is presented in Fig. 5B. There is a linear relation between response current and H_2O_2 concentration in the range of 0–5.35 mM with a sensitivity of 4.844 μA mM^{-1} (or 80.74 μA mM^{-1} cm^{-2}) (the linear fitting correction coefficient $R = 0.9986$), while for a higher concentration of H_2O_2, the plot deviates from linearity, which may be attributed to the saturation of the electrocatalytic activity of Co_3O_4 nanowalls. Compared to the detection operated at an applied potential of +0.8 V, the most appealing aspect for the applied potential of −0.2 V is that a lot of interferences can be substantially eliminated. Various H_2O_2 sensors have been reported in literature. However, it is very difficult to compare one sensor to others because the performance of the sensor is greatly dependent on the applied potential, the use of rotating electrode or static electrode, the supporting electrolyte, and the electrode material (GC, Pt, gold, etc.) and its surface area. To the best of our efforts, various H_2O_2 sensors are summarized in Table 1 with respect to the operating conditions, sensitivity, and the detection limit. It can be seen that the performance of the developed sensor is comparable to most of H_2O_2 sensors in literature in one or more categories.

Metal oxides have unique advantages in electrochemical detection of different analytes. Nafion and CuO nanoparticles, cobalt oxide–porphyrin composites, and Co_3O_4 nanoparticle–carbon black have been used to modify electrodes for H_2O_2 reduction in strong basic NaOH solution [11,47,48]. In these studies, metal oxides entrapped in a matrix suffer from strong diffusion resistance offered by the entrapment material. The use of a strong NaOH solution also limits their further application in biosensor development because most of biomolecules can not survive under such harsh environment. In addition, the fabrication of these electrodes involves complicated and time-consuming procedures. Recently, directly electrodeposited Co_3O_4 nanoparticles on a rotating GC electrode was reported for H_2O_2 detection at +0.75 V (vs. Ag/AgCl) [1]. However, its application may be limited by the use of rotating electrode and the further work required for uniformity of particles and for decreasing their size. As a comparison, the Co_3O_4 nanowalls used in this study can be easily synthesized as a film with any size, manipulated by scissors and tweezers, and attached to any electrode surface using conductive paint. In addition, the vertically aligned Co_3O_4 nanowalls form a porous structure and possess high specific surface area, allowing the access of analytes to the cobalt oxide surface with minimal diffusion resistance. Moreover, the single crystalline Co_3O_4 nanowalls have good conductivity, which provide many transport channels in nanoscale, and thus, enhance the

Table 1
Comparison of various H_2O_2 sensors.

Electrode modifier (electrode)	Applied potential (V vs. Ag/AgCl)	Electrolyte	Sensitivity (μA/mM)	Detection limit (μM)	Reference
Co_3O_4 nanowalls (GC)	−0.2	0.01 M pH 7.4 phosphate	4.844 (or 80.74[b])	10	This study
	+0.8		100.3 (or 1671[b])	2.8	
Ru/Rh (gold)	−0.1	0.2 M phosphate + 0.2 M KCl	1.060	1	[39]
Fe_3O_4/Chitosan (GC rotating electrode)	−0.2	pH 7 solution	9.6	7.4	[51]
DNA-Cu(II) (GC)	−0.2	0.05 M pH 5 phosphate	12.8	0.05	[52]
DNA-Cu(II) poly(amine) (GC)	−0.2	0.05 M pH 5 phosphate	12.8	0.05	[53]
Prussian blue-PAMAM (gold)	−0.2 (vs. SCE)	0.1 M pH 6.5 phosphate	93.2[a]	0.31	[45]
Nafion-nano CuO (Pt)	−0.3 (vs. SCE)	0.1 M NaOH	–	0.06	[48]
Polyaniline grafted MWNT (ITO)	−0.3 (vs. SCE)	pH 7 phosphate	300	0.001	[36]
Nano-Ag + DNA networks (GC)	−0.4 (vs. SCE)	0.2 M pH 7 phosphate	–	1.7	[54]
Gold nanoparticle–silca sol–gel (GC)	−0.5 (vs. SCE)	0.1 M pH 7 phosphate	30	3.15×10^{-3}	[55]
Poly(p-aminobenzene sulfonic acid) (GC rotating electrode)	−0.7	0.1 M pH 7 phosphate	100[a]	10	[56]
Iodide (gold)	−1.1	0.1 M KOH + 12.5 mM KI	5.47[a]	10	[41]
RuO-hexacyanoferrate (GC)	0	0.5 M KCl + 0.05 M HCl	1.8	1.3	[57]
Prussian blue (GC)	+0.05	0.1 M HCl + 0.1 M KCl	1.884[a]	0.01	[58]
CeO_2 (gold)	+0.2	DI H_2O	0.4806	1	[40]
Nano-TiO_2 and Pt (Ti foil)	+0.3	0.05 M pH 7.4 phosphate + 0.1 M NaCl	0.85	4	[59]
Cobalt oxide/CoTRP (GC)	+0.3	0.5 M NaOH	–	0.2	[11]
Nano-MnO_2 (carbon paste electrode)	+0.3	0.01 M pH 7.4 phosphate buffer	–	2	[60]
MnO_2 (carbon paste electrode)	+0.46	0.2 M NH_3–NH_4Cl buffer	33.15	1.32	[61]
Ferrocene peapod-modified SWNT (GC)	+0.5 (vs. SCE)	0.1 M $LiClO_4$ + 25 mM pH 7.2 phosphate	–	5	[42]
Pt-implanted (boron-doped diamond electrode)	+0.55	0.1 M pH 7 phosphate	21.9	0.03	[35]
Mesoporous Pt (Pt)	+0.6 (vs. SCE)	0.1 M pH 7 phosphate	2800[b]	4.5	[38]
Nano-MnO_2 + DHP (GC)	+0.65 (vs. SCE)	0.067 M pH 7.4 phosphate buffer	20.35[a]	0.08	[62]
Carbon nanofiber (GC)	+0.65	0.05 M pH7.4 phosphate buffer + 0.1 M NaCl	3.20	4	[63]
MnO_2 graphite composite (paste electrode)	+0.75 (vs. SCE)	pH 7 phosphate	–	1.5	[64]
Cobalt oxide nanoparticles (GC rotating electrode)	+0.75	0.1 M pH 7 phosphate	152.6[a]	4×10^{-4}	[1]
Carbon nanotubes (CNT paste electrode)	+0.95	0.2 M pH 7 phosphate buffer	0.8	20	[65]

[a] Calculated from the data in paper.
[b] In μA/mM cm^2.

electron-transfer reaction between H_2O_2 and the Co_3O_4 nanowalls. All these features provide a favorable environment for the electrocatalytic oxidation and reduction of H_2O_2 and allow the sensitive detection of H_2O_2 at both positive and negative applied potentials and at physiological pH, which makes it more appealing than other metal oxide nanoparticles in sensor and biosensor applications.

4. Conclusion

Single crystal and vertically aligned Co_3O_4 nanowalls were synthesized by directly heating Co foil on a hot-plate under ambient conditions. The electrocatalytic property of Co_3O_4 nanowalls electrode was investigated using H_2O_2 as a model compound. We have demonstrated that the Co_3O_4 nanowalls electrode, compared to the bare GC electrode, exhibits significantly lower overpotentials for oxidation and reduction of H_2O_2 in 0.01 M pH 7.4 phosphate buffer solutions. The electrocatalytic oxidation and reduction of H_2O_2 at the vertically aligned Co_3O_4 nanowalls electrode offers a number of attractive features. The as-grown Co_3O_4 nanowalls film is mechanically stable and can be used directly as electrochemical sensor for H_2O_2 detection. The Co_3O_4 nanowalls electrode showed a fast response and high sensitivity for H_2O_2 at applied potentials of +0.8 V and −0.2 V (vs. Ag/AgCl), respectively. Specifically, the sensitive detection of H_2O_2 based on strong reduction at a negative applied potential has the potential to eliminate the interferences from other electroactive compounds. These results demonstrate that Co_3O_4 nanowalls have great potential in sensor and biosensor applications.

Acknowledgment

We greatly appreciate the funding from UConn large faculty research grant and NSF (CMMI 0730826).

References

[1] A. Salimi, R. Hallaj, S. Soltanian, H. Mamkhezri, Anal. Chim. Acta 594 (2007) 24.
[2] Y. Usui, K. Sato, M. Tanaka, Angew. Chem. Int. Ed. 42 (2003) 5623.
[3] N.A. Choudhury, R.K. Raman, S. Sampath, A.K. Shukla, J. Power Sources 143 (2005) 1.
[4] S. Hasegawa, K. Shimotani, K. Kishi, H. Watanabe, Electrochem. Solid State Lett. 8 (2005) A119.
[5] T. Kim, J.S. Hwang, S. Kwon, Lab. Chip 7 (2007) 835.
[6] E. Kjeang, A.G. Brolo, D.A. Harrington, N. Djilali, D. Sinton, J. Electrochem. Soc. 154 (2007) B1220.
[7] G.H. Miley, N. Luo, J. Mather, R. Burton, G. Hawkins, L.F. Gu, E. Byrd, R. Gimlin, P.J. Shrestha, G. Benavides, J. Laystrom, D. Carroll, J. Power Sources 165 (2007) 509.
[8] R.K. Raman, A.K. Shukla, Fuel Cells 7 (2007) 225.
[9] A. Ramanavicius, A. Kausaite, A. Ramanaviciene, Biosens. Bioelectron. 20 (2005) 1962.
[10] L. Campanella, R. Roversi, M.P. Sammartino, M. Tomassetti, J. Pharm. Biomed. Anal. 18 (1998) 105.
[11] M.S.M. Quintino, H. Winnischofer, K. Araki, H.E. Toma, L. Angnes, Analyst 130 (2005) 221.
[12] S. Cosnier, S. Szunerits, R.S. Marks, A. Novoa, L. Puech, E. Perez, I. Rico-Lattes, Electrochem. Commun. 2 (2000) 851.
[13] M.D. Gouda, M.A. Kumar, M.S. Thakur, N.G. Karanth, Biosens. Bioelectron. 17 (2002) 503.
[14] D. Shan, M.J. Zhu, H.G. Xue, S. Cosnier, Biosens. Bioelectron. 22 (2007) 1612.
[15] M.C. Shin, H.S. Kim, Biosens. Bioelectron. 11 (1996) 161.
[16] J.X. Wang, X.W. Sun, A. Wei, Y. Lei, X.P. Cai, C.M. Li, Z.L. Dong, Appl. Phys. Lett. 88 (2006) 233106.
[17] A. Wei, X.W. Sun, J.X. Wang, Y. Lei, X.P. Cai, C.M. Li, Z.L. Dong, W. Huang, Appl. Phys. Lett. 89 (2006) 123902.
[18] I. Willner, A. Riklin, B. Shoham, D. Rivenzon, E. Katz, Adv. Mater. 5 (1993) 912.
[19] Y.J. Zou, C.L. Xiang, L.X. Sun, F. Xu, Biosens. Bioelectron. 23 (2008) 1010.
[20] N.V. Klassen, D. Marchington, H.C.E. Mcgowan, Anal. Chem. 66 (1994) 2921.
[21] A.M. Almuaibed, A. Townshend, Anal. Chim. Acta 295 (1994) 159.
[22] P.A. Tanner, A.Y.S. Wong, Anal. Chim. Acta 370 (1998) 279.
[23] M. Zhu, X.M. Huang, L.Z. Liu, H.X. Shen, Talanta 44 (1997) 1407.
[24] I. Mori, K. Takasaki, Y. Fujita, T. Matsuo, Talanta 47 (1998) 631.
[25] R. Rapoport, I. Hanukoglu, D. Sklan, Anal. Biochem. 218 (1994) 309.
[26] A. Sakuragawa, T. Taniai, T. Okutani, Anal. Chim. Acta 374 (1998) 191.
[27] T. Taniai, A. Sakuragawa, T. Okutani, Anal. Sci. 15 (1999) 1077.
[28] M.J. Zhou, Z.J. Diwu, N. PanchukVoloshina, R.P. Haugland, Anal. Biochem. 253 (1997) 162.
[29] A.N. Diaz, M.C.R. Peinado, M.C.T. Minguez, Anal. Chim. Acta 363 (1998) 221.
[30] K. Okamura, T. Gamo, H. Obata, E. Nakayama, H. Karatani, Y. Nozaki, Anal. Chim. Acta 377 (1998) 125.
[31] J.C. Yuan, A.M. Shiller, Anal. Chem. 71 (1999) 1975.
[32] S. Effkemann, U. Pinkernell, U. Karst, Anal. Chim. Acta 363 (1998) 97.
[33] U. Pinkernell, S. Effkemann, U. Karst, Anal. Chem. 69 (1997) 3623.
[34] J.G. Hong, J. Maguhn, D. Freitag, A. Kettrup, Fresen. J. Anal. Chem. 361 (1998) 124.
[35] T.A. Ivandini, R. Sato, Y. Makide, A. Fujishima, Y. Einaga, Diam. Relat. Mater. 14 (2005) 2133.
[36] P. Santhosh, K.M. Manesh, A. Gopalan, K.P. Lee, Anal. Chim. Acta 575 (2006) 32.
[37] Y. Shen, M. Trauble, G. Wittstock, Anal. Chem. 80 (2008) 750.
[38] S.A.G. Evans, J.M. Elliott, L.M. Andrews, P.N. Bartlett, P.J. Doyle, G. Denuault, Anal. Chem. 74 (2002) 1322.
[39] D. Janasek, W. Vastarella, U. Spohn, N. Teuscher, A. Heilmann, Anal. Bioanal. Chem. 374 (2002) 1267.
[40] A. Mehta, S. Patil, H. Bang, H.J. Cho, S. Seal, Sens. Actuat. A 134 (2007) 146.
[41] R. Miah, T. Ohsaka, Anal. Chem. 78 (2006) 1200.
[42] N.J. Sun, L.H. Guan, Z.J. Shi, N.Q. Li, Z.N. Gu, Z.W. Zhu, M.X. Li, Y.H. Shao, Anal. Chem. 78 (2006) 6050.
[43] J. Tkac, T. Ruzgas, Electrochem. Commun. 8 (2006) 899.
[44] Y. Wang, W.Z. Wei, J.X. Zeng, X.Y. Liu, X.D. Zeng, Microchim. Acta 160 (2008) 253.
[45] S.G. Wu, T.L. Wang, C.Q. Wang, Z.Y. Gao, C.Q. Wang, Electroanalysis 19 (2007) 659.
[46] T.Y. You, O. Niwa, M. Tomita, S. Hirono, Anal. Chem. 75 (2003) 2080.
[47] D.X. Cao, J.D. Chao, L.M. Sun, G.L. Wang, J. Power Sources 179 (2008) 87.
[48] X.M. Miao, R. Yuan, Y.Q. Chai, Y.T. Shi, Y.Y. Yuan, J. Electroanal. Chem. 612 (2006) 157.
[49] T. Yu, Y.W. Zhu, X.J. Xu, Z.X. Shen, P. Chen, C.T. Lim, J.T.L. Thong, C.H. Sow, Adv. Mater. 17 (2005) 1595.
[50] T. Yu, Y.W. Zhu, X.J. Xu, K.S. Yeong, Z.X. Shen, P. Chen, C.T. Lim, J.T.L. Thong, C.H. Sow, Small 2 (2006) 80.
[51] M.S. Lin, H.J. Len, Electroanalysis 17 (2005) 2068.
[52] Y. Hasebe, T.T. Gu, J. Electroanal. Chem. 576 (2005) 177.
[53] T.T. Gu, Y. Hasebe, Biosens. Bioelectron. 21 (2006) 2121.
[54] K. Cui, Y.H. Song, Y. Yao, Z.Z. Huang, L. Wang, Electrochem. Commun. 10 (2008) 663.
[55] G. Maduralveeran, R. Ramaraj, J. Electroanal. Chem. 608 (2007) 52.
[56] S.A. Kumar, S.M. Chen, J. Mol. Catal. A: Chem. 278 (2007) 244.
[57] T.R.L.C. Paixao, M. Bertotti, Electroanalysis 20 (2008) 1671.
[58] A.A. Karyakin, E.A. Puganova, I.A. Budashov, I.N. Kurochkin, E.E. Karyakina, V.A. Levchenko, V.N. Matveyenko, S.D. Varfolomeyev, Anal. Chem. 76 (2004) 474.
[59] X.L. Cui, Z.Z. Li, Y.C. Yang, W. Zhang, Q.F. Wang, Electroanalysis 20 (2008) 970.
[60] Y.H. Lin, X.L. Cui, L.Y. Li, Electrochem. Commun. 7 (2005) 166.
[61] K. Schachl, H. Alemu, K. Kalcher, J. Jezkova, I. Svancara, K. Vytras, Analyst 122 (1997) 985.
[62] S.J. Yao, J.H. Xu, Y. Wang, X.X. Chen, Y.X. Xu, S.S. Hu, Anal. Chim. Acta 557 (2006) 78.
[63] Z.Z. Li, X.L. Cui, J.S. Zheng, Q.F. Wang, Y.H. Lin, Anal. Chim. Acta 597 (2007) 238.
[64] B. Sljukic, R.G. Compton, Electroanalysis 19 (2007) 1275.
[65] F. Valentini, A. Amine, S. Orlanducci, M.L. Terranova, G. Palleschi, Anal. Chem. 75 (2003) 5413.